284–289 *Nucleic Acids Research, 2012, Vol. 40, No. 1* *Published online 6 September 2011*
doi:10.1093/nar/gkr712

How environmental solution conditions determine the compaction velocity of single DNA molecules

Ken Hirano[1,*], Masatoshi Ichikawa[2], Tomomi Ishido[1], Mitsuru Ishikawa[1], Yoshinobu Baba[1,3] and Kenichi Yoshikawa[2,*]

[1]Health Research Institute, National Institute of Advanced Industrial Science and Technology (AIST), Hayashi-cho, Takamatsu, Kagawa, 761-0395, [2]Department of Physics, Kyoto University, Sakyo-ku, Kyoto, 606-8502 and [3]Department of Applied Chemistry, Nagoya University, Chikusa-ku, Nagoya, 464-8603, Japan

Received June 21, 2011; Revised and Accepted August 18, 2011

ABSTRACT

Understanding the mechanisms of DNA compaction is becoming increasingly important for gene therapy and nanotechnology DNA applications. The kinetics of the compaction velocity of single DNA molecules was studied using two non-protein condensation systems, poly(ethylene glycol) (PEG) with Mg^{2+} for the polymer-salt-induced condensation system and spermine for the polyamine condensation system. The compaction velocities of single tandem λ-DNA molecules were measured at various PEG and spermine concentrations by video fluorescent microscopy. Single DNA molecules were observed using a molecular stretching technique in the microfluidic flow. The results show that the compaction velocity of a single DNA molecule was proportional to the PEG or spermine concentration to the power of a half. Theoretical considerations indicate that the compaction velocity is related to differences in the free energy of a single DNA molecule between the random coil and compacted states. In the compaction kinetics with PEG, acceleration of the compaction velocity occurred above the overlap concentration while considerable deceleration occurred during the coexistence state of the random coil and the compacted conformation. This study demonstrates the control factors of DNA compaction kinetics and contributes toward the understanding of the compaction mechanisms of non-protein DNA interactions as well as DNA–protein interactions *in vivo*.

INTRODUCTION

DNA, the carrier of genes, is a long chain 2 nm thick and ~50 nm in persistence length. A typical DNA chain in a living cell is on the order of several tens of kilobase pairs giving it a 'semiflexible polymer' nature. In a simple model system using nude DNA molecules, it has been revealed that a single DNA molecule exhibits a first-order type phase transition of higher order structure from a random coil to a tightly packed state by using various condensing agents (1–16). Even in such simple model systems, a compacted or condensed state of DNA can inhibit RNA transcription activity (17). The primary processes in the compaction of a single DNA molecule have been observed by fluorescence microscopy (3–6,18,19). However, the compaction kinetics, especially the compaction velocity, of a single DNA molecule is still a topic of intense research.

The density transition of DNA in bulk is known as DNA condensation (1). To elucidate the compaction mechanism of DNA molecules *in vivo*, the process has been studied *in vitro* using various condensing reagents such as proteins, polyamines, hexamine cobalt(III) complexes and cationic surfactants (1–8). These agents are components of the nucleus or nucleoid, and are representative models of the environment of biological organisms. Additionally, in models of crowding environments or intracellular environments, poly(ethylene glycol) (PEG) has been used for a polymer-salt-induced (ψ) condensation system (10,20,21). All living organisms contain a wide variety of macromolecules that may reach a total concentration of 50–400 mg/ml. To mimic molecular crowding *in vitro*, PEG has been commonly used as a large cosolute (22), as has albumin under low salt conditions (16).

Static structures and characteristics of the compacted DNA have been observed by various methods. Electron microscopy shows that compacted DNA *in vivo* and *in vitro* assumes an ordered form (9–11). Light scattering techniques have revealed ensemble behavior of DNA compaction (1–23). In contrast to static observations, research on the compaction dynamics of single DNA molecules have been carried out on cellular proteins (3–6). Despite being the subject of active research, however, information

*To whom correspondence should be addressed. Tel/Fax: +81 87 869 3569; Email: hirano-ken@aist.go.jp
Correspondence may also be addressed to Kenichi Yoshikawa. Tel: +81 75 753 3749; Fax: +81 75 753 3779; Email: yoshikaw@scphys.kyoto-u.ac.jp

on the kinetics of the DNA compaction has not been clearly delineated at the level of a single molecule. Especially, quantitation of the compaction velocity is important because it relates to cell division, sperm manufacturing and gene expression control. However, using a protein condensation system as a theoretical model for analysis of DNA compaction velocity is difficult due to the complexity of the chemical and biochemical characteristics of the proteins as compaction components.

In the present study, to evaluate the compaction kinetics or compaction velocity of a single DNA molecule in detail we first investigated non-protein condensation systems using (i) PEG with Mg^{2+}, which exhibits a crowding effect suitable for mimicking cellular fluid, as the ψ condensation system and (ii) spermine (SPM), which is present in living cells at high concentrations, as the polyamine condensation system.

MATERIALS AND METHODS

Bead–avidin complex

The carboxyl-polystyrene beads (Polysciences, Inc. Valley Road, USA) with a diameter of 1 μm were washed twice with 50 mM 2-(*N*-morpholino)ethanesulfonic acid (MES) buffer pH 5.2 and then re-suspended in MES buffer. To ensure rapid reaction with the amine group, 20 mg/ml 1-ethyl-3-(dimethylaminopropyl) carbodiimide hydrochloride (EDC; Thermo Fisher Scientific, Bonn, Germany) was added to the bead solution, and the mixture was agitated for 4 h at room temperature. An appropriate volume of dissolved 20 μg/μl streptavidin (Sigma-Aldrich) was added to the EDC–bead mixture, and incubated and stirred overnight at room temperature. The bead–avidin complex was recovered by removing the supernatant following centrifugation at 2000*g* for 5 min. The bead–avidin complex was re-suspended in storage buffer (10 mM Tris pH 8.0, 0.05% BSA) at 4°C before use.

Biotinylated λDNA concatemers

Double-stranded lambda phage DNA was purchased from Takara (Shiga, Japan). Concatemers of lambda DNA were prepared with T4 DNA ligase (Takara, Shiga, Japan) by incubating in ligation buffer for 1 h at 25°C. To biotinylate one end of the concatemeric DNA, a biotin-labeled oligonucleotide with the sequence 5′-GGG CGGCGACCT-biotin-3′ (Sigma-Aldrich), which is hybridized at the right cos site of lambda phage DNA, was added to the concatemeric DNA solution at a DNA:oligonucleotide ratio of 1:2 and incubated for 10 min at room temperature with T4 DNA ligase. After ligation of the biotin-labeled oligonucleotide, the concatemeric biotinylated DNA was isolated by 1% agarose gel electrophoresis in 1× TAE and extracted from gel slices by electro-elution.

Compaction velocity measurement

To investigate the compaction velocity of single DNA molecules, we used a microfluidic chip made from polydimethylsiloxane (PDMS) for observation, which has one main microchannel (4-mm wide, 25-μm deep) and four branch channels (1-mm wide, 25-μm deep) (Figure 1a). All solutions from each branch channel were pumped with electro-osmotic pumps (Nano Fusion Technologies, Tokyo, Japan). The following procedures were conducted at room temperature (~23–25°C). First, the bead–avidin complex was injected into the main channel for 5 min at a flow rate of ~15 μm/s, and then washed with buffer (5 mM MOPS buffer, pH 7.4). The biotinylated lambda DNA concatemer subsection below) was injected into the channel for 5 min at a flow rate of ~15 μm/s, fixed to the bead–avidin complex spacers and washed with buffer. The condensing reagents of PEG–Mg^{2+} (60 mM $MgCl_2$ and 0–120 mg/ml PEG 6000 [Hampton Research]) and SPM [0–20 μM SPM (Nacalai Tesque, Kyoto, Japan)] in 50 mM MOPS pH 7.4 were injected into the main channel at a flow rate of 25–40 μm/s. DNA molecules were stained and visualized with fluorescence dye DAPI (4′,6-diamidino-2-phenylindole, 0.6 μM). An EB–CCD camera with a fluorescence microscope captured the kinetic process. The length and velocity of DNA were analyzed using the Meta Imaging Software (Molecular Devices, USA).

Measurement of viscosity from Brownian motion

For measurement of viscosity, the Brownian motion of a polystyrene 500-nm bead was measured by fluorescence microscopy, and the time-dependent translational displacement of an individual bead was quantified to estimate viscosity using the Stokes–Einstein equation (8). Single particle tracking for the measurement of microscopic viscosity was carried out in the aforementioned buffer solutions containing 0–140 mg/ml PEG without Mg^{2+}.

RESULTS AND DISCUSSION

We measured the compaction velocity of single tandem λ-DNA molecules with contour lengths of ~20–70 μm by video fluorescent microscopy. Single DNA molecules were observed using a molecular stretching technique in the microfluidic flow. Figure 1a shows a schematic of the experimental setup. The compaction is induced by the exchange of buffer solution for condensing solution in the channel. Figure 1b and c as well as Supplementary Movies S1 and S2 show a time lapse for compaction of a single DNA molecule. To keep a single DNA molecule from unexpected adhesion on the glass surface during the compaction, we immobilized it on a microbead as a spacer. First, a microbead coated with streptavidin was nonspecifically immobilized on the glass surface, and then a single DNA molecule labeled with biotin was bound on the microbead via the avidin–biotin linkage. Moreover, the flow rate in the present study was selected on the range of 25–40 μm/s, which corresponds to the flow rates adapted in previous studies (3–6). We avoided stronger flow to prevent additional nonlinear effects on the transition.

We observed the compaction velocity of a single DNA molecule at various PEG and SPM concentrations. Figure 2a and b shows that the shrinkage of a single DNA

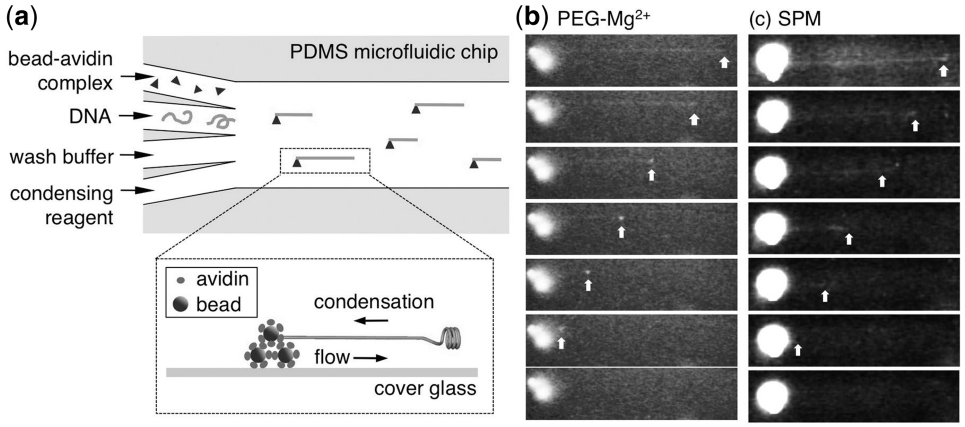

Figure 1. Single molecule compaction of DNA. (**a**) Schematic of experimental setup. Single DNA molecules were immobilized with one end of the DNA on microbeads as a spacer, and stretched by continuous laminar flow in a microfluidic channel. Time lapse of compaction by (**b**) 100 mg/ml PEG and 60 mM $MgCl_2$ and (**c**) 20 μM SPM. The arrows indicate the end of a single DNA molecule during DNA compaction. The time intervals between images for (b) and (c) are 0.13 and 0.03 s, respectively.

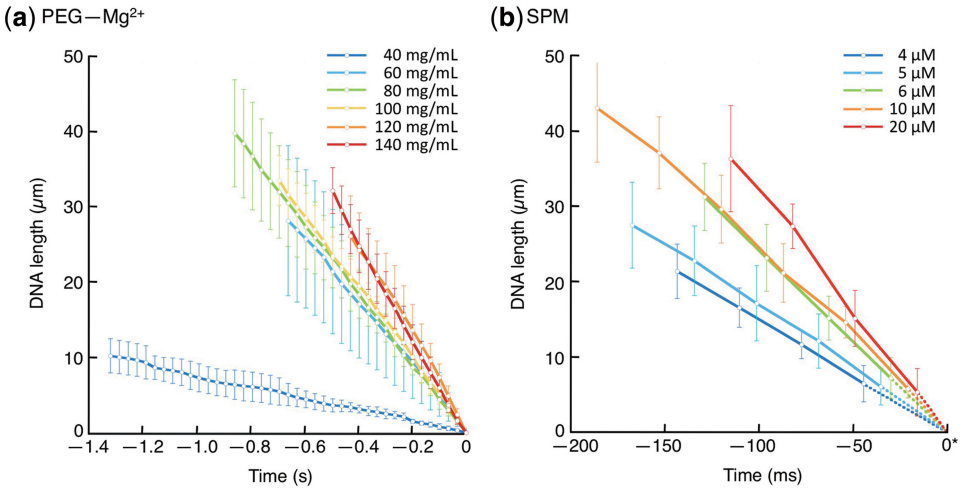

Figure 2. Time lapse of the length of a single DNA molecule induced by (**a**) PEG–Mg^{2+} (60 mM $MgCl_2$ and 40–140 mg/ml PEG) and (**b**) SPM (4–20 μM). Time 0 is the time at which compaction was complete. Each data point was obtained by averaging over five molecules at each bin time in the video frame. A smaller number of data points are plotted for SPM owing to its faster velocity of compaction. Time 0* for SPM is the expected complete time of the compaction, which was evaluated from the time-successive video frames with the time interval of 33 ms.

molecule was approximately linear at each concentration, and the velocity of shrinkage increased with increasing concentrations of condensing reagents. Figure 3a and b shows that the maximum averaged compaction velocity induced by PEG–Mg^{2+} and SPM was ~60 μm/s (i.e. ~180 kb/s) and ~350 μm/s (i.e. ~1 Mb/s), respectively. The velocity is faster than that induced by protein by a factor of 5–30 (3–6). The transition time in millisecond order by the SPM compaction was similar to that in fluorescence lifetime correlation spectroscopic study (24). Figure 3a and b also shows that threshold concentrations were found in DNA compaction, reflecting the intrinsic nature of the transition on single DNA (24,25). In other words the compaction is mediated under the excess concentration of SPM and the ruling kinetics is growth process after the nucleation. Whereas with protamine, Brewer *et al*. reported that the compaction velocity is proportional to the protein concentration, which is interpreted in terms of the kinetics of protamine binding. Single DNA molecules were not compacted in [PEG] <20 mg/ml, however, were completely compacted above the threshold concentration of [PEG] >60 mg/ml. Thus, the threshold concentration was [PEG] = 60 mg/ml. At [PEG] = 40 mg/ml, a single DNA molecule in a random coil and in a compacted state were simultaneously observed (fluorescence images in Figure 3a). Under these coexisting conditions, a few molecules were compacted and had compaction velocities slower than under the completely compacted conditions at [PEG] >60 mg/ml. The single DNA molecules remains as the elongated coil state without Mg^{2+} at the PEG concentration adapted in this study (data not shown). Although the experiments

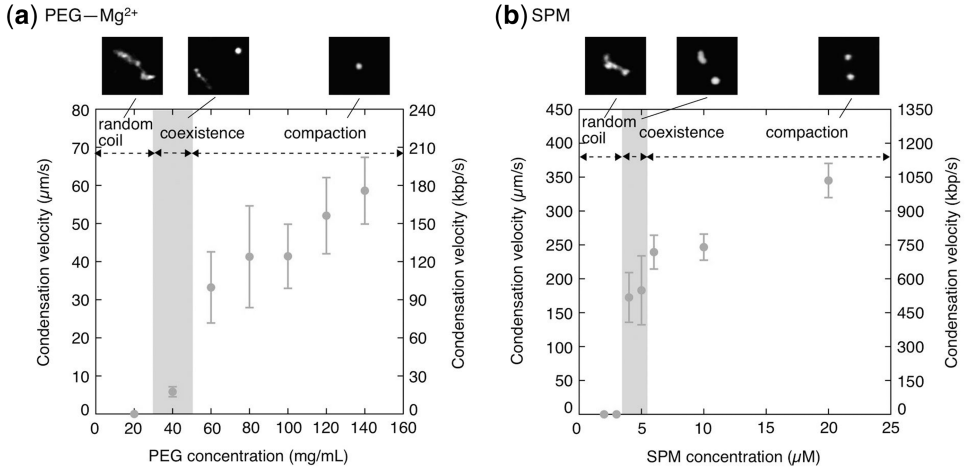

Figure 3. Velocity of compaction of single DNA molecules. (**a**) PEG–Mg^{2+} (60 mM $MgCl_2$, constant) and (**b**) SPM. Each photograph in the above graphs was observed without liquid flow and by anchoring single DNA molecules to examine their conformation state in the presence of varying reagent concentrations using fluorescence microscopy. Each data point was obtained by averaging over five molecules except at [PEG] = 40 mg/ml in (a), where averaging was done over four molecules owing to difficulties in observing a small number of condensed molecules in the coexistence region.

with SPM exhibited a tendency similar to those with PEG–Mg^{2+}, the velocity was higher than in the presence of PEG–Mg^{2+} (Figures 2, 3, Supplementary Movies S1 and S2). A threshold concentration of SPM was also required to induce complete DNA compaction (Figure 3b). At [SPM] = 4–5 μM, random coil and compacted conformations of single DNA molecules were simultaneously observed (fluorescence images in Figure 3b). DNA molecules were not compacted in [SPM] <3 μM, however, were completely compacted in [SPM] >6 μM. Thus, the threshold concentration was [SPM] = 6 μM.

The velocity v of shrinkage of a single DNA molecule is $v \sim \sqrt{D/\tau}$ in a general model of phase propagation, or nucleation-growth model (25). D is a diffusion coefficient associated with viscosity η from $D \propto 1/\eta$; t is the time scale of the local kinetics in the compaction. The local kinetics follows: $1/\tau \propto dx/dt \propto \exp(-E_a/kT)$, where E_a is the local activation energy for the compaction of the DNA segments between the random coil and compacted states. We assumed that the activation energy E_a is proportional to the difference in free energy DF on a single DNA molecule between the random coil and compacted states: $E_a \sim$ DF. As for the free energy expression as the function of [SPM], several studies have appeared (25–27). By adapting the main factor, we may expect that ΔF is nearly proportional to kTIn[SPM] to be near the critical concentration of the condensing reagents (25). Thus,

$$v^2 \propto \frac{[\mathrm{SPM}]}{\eta}. \quad (1)$$

Based on Equation (1), we may expect the relationship, $v \propto [\mathrm{SPM}]^{0.5}$, under the constant η. In the compaction by SPM, η is assumed to be constant and almost equal to the viscosity of water. The experimental results in Figures 2b and 4a show constant velocity and $v \propto [\mathrm{SPM}]^{0.5}$ with $R = 0.98$, the coefficient for least squares fitting. Thus, the experimental results were well fit to Equation (1).

Dependence of the compaction velocity on PEG is different from that of SPM owing to the fact that the viscosity of a PEG solution is higher than that of a SPM solution. Thus, we examined the viscosity of the PEG solution by tracking single nanoparticles in Brownian motion at various [PEG]. Figure 4b shows that the overlap concentration of the PEG polymers was found at ~95 mg/ml from the turning point of the viscosity.

We investigated the relationship between velocity and viscosity by plotting $v^2\eta$ against [PEG] and [SPM]. Figure 4a shows that the rate with SPM is given as $v \propto [\mathrm{SPM}]^{0.5}$. On the other hand, with PEG the rate is expressed as $v \propto [\mathrm{PEG}]^{0.5}$ and $v \propto [\exp([\mathrm{PEG}]^{9/4})]^{0.5}$ below and above the overlap concentration, respectively. The 9/4 power of [PEG] comes from the osmotic pressure of the polymer (28). The slope and the magnitude of $v^2\eta$ depends on PEG–Mg^{2+} or SPM owing to their different viscosities and chemical properties. The driving force for compaction is the depletion of PEG between the DNA segments (20), which originates in the entropy gain of PEG during the decrease in the effective free volume of the DNA molecule. Thus, the difference in the free energy for the DNA segments between random coil and compacted states E_a is proportional to PEG concentration below the overlap concentration. However, our results suggest that two theoretical models for the compaction velocity of a single DNA molecule are required for the situations below and above the overlap concentration of PEG.

The critical concentration for transition between the random coil and compacted states of single DNA molecules, where the free energy is equal between the two states, was estimated at [SPM] = 0.75 μM from the x-intercept of the fitted line in the $v -$ In[SPM] plot (Supplementary Figure S1). However, the compaction

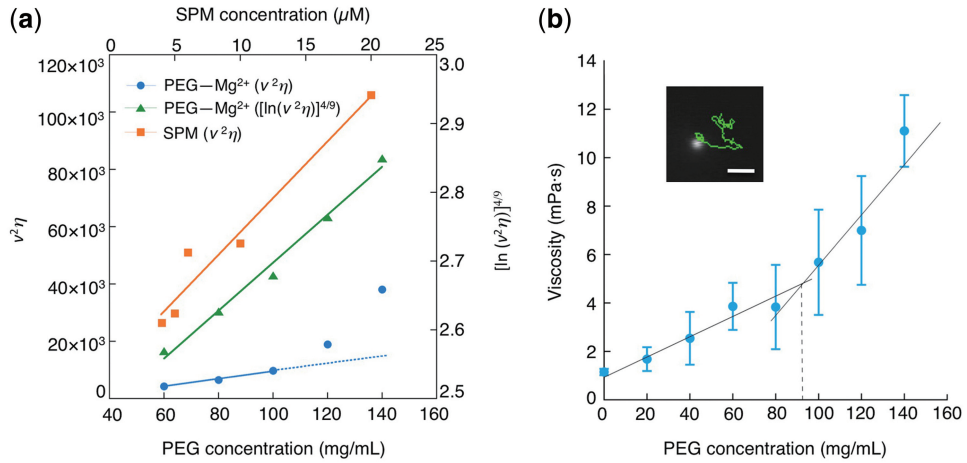

Figure 4. Relationship of compaction velocity to concentration of condensing reagent and solution viscosity. (**a**) Relationship of compaction velocity to the concentration for PEG–Mg^{2+} and SPM. (**b**) Viscosity calculated from tracking a single 500-nm particle in Brownian motion (inset) as a function of PEG concentration. Scale bar in the inset is 3 μm.

starts from the threshold concentration reflecting the intrinsic nature of the transition on single DNA described above, not from the critical concentration. The attraction factor (i.e. the concentration of SPM) must be greater than that at the critical concentration. This requirement means that the attraction force between the DNA segments or the velocity of the compaction becomes faster than that at the critical concentration. Thus, we predict a lower velocity of compaction near the critical point in continuous transitions, or second-order transitions of DNA. The observation of compaction in the presence of protein exhibits a continuous transition of DNA (3–6). Thus, we predict that compaction using protein causes low-velocity compaction compared with that by SPM and PEG–Mg^{2+}.

For compaction by PEG–Mg^{2+}, a critical concentration for transition between the random coil and the compacted states of single DNA molecules is observed in the overlap regime (20). The driving force for compaction is the depletion force caused by the change in effective free volume to increase the PEG–PEG and DNA–DNA interactions rather than the DNA–PEG interaction above the overlap concentration. The critical concentration decreases with increasing salt concentration (20). Indeed, the threshold of [PEG] for DNA compaction at 60 mg/ml in Figure 3a was different from the overlap concentration at 95 mg/ml in Figure 4b.

In conclusion, we have demonstrated for the first time the kinetics of the structural transition due to DNA compaction from direct evidence of the observation of single DNA molecules. The phase propagation model explains the kinetics measured using non-protein-induced compactions in the presence of PEG–Mg^{2+} and SPM. We experimentally identified $v \propto [\text{PEG or SPM}]^{0.5}$ and theoretical considerations indicated that the compaction velocity was related to the difference in free energy of a single DNA molecule between the random coil and compacted states. In the compaction kinetics with PEG, acceleration of the compaction velocity occurred above the overlap concentration, and considerable deceleration was observed during the coexistence state of random coil and the compacted conformation. The experimental results indicate that the compaction kinetics are controlled by the viscosity of the condensing reagents and the difference in free energy of a single DNA molecule between random coil and compacted states by considering the underlying properties of the entire genomic DNA. Our present work, which demonstrates the control factors of DNA compaction kinetics, should support important progress towards disclosing the compaction mechanisms of not only non-protein DNA interactions but also DNA–protein interactions *in vivo*. Furthermore, the control factors of compaction discussed herein support the ideas that they contribute not only to RNA transcription control (17) but also are important for applications of artificial compaction for gene therapy (11) and nanotechnology (13,14).

SUPPLEMENTARY DATA

Supplementary Data are available at NAR Online.

FUNDING

Industrial Technology Research Program from the New Energy and Industrial Technology Development Organization (NEDO), Japan. Funding for open access charge: New Energy and Industrial Technology Development Organization.

Conflict of interest statement. None declared.

REFERENCES

1. Bloomfield,V.A. (1996) DNA condensation. *Curr. Opin. Struct. Biol.*, **6**, 334–341.
2. Besteman,K., Van Eijk,K. and Lemay,S.G. (2007) Charge inversion accompanies DNA condensation by multivalent ions. *Nat. Phys.*, **3**, 641–644.

3. Brewer,L.R., Corzett,M. and Balhorn,R. (1999) Protamine-induced condensation and decondensation of the same DNA molecule. *Science*, **286**, 120–123.
4. Brewer,L.R., Corzett,M. and Balhorn,R. (2002) Condensation of DNA by spermatid basic nuclear proteins. *J. Biol. Chem.*, **277**, 38895–38900.
5. Brewer,L.R., Friddle,R., Noy,A., Baldwin,E., Martin,S.S., Corzett,M., Balhorn,R. and Baskin,R.J. (2003) Packaging of Single DNA Molecules by the Yeast Mitochondrial Protein Abf2p. *Biophys. J.*, **85**, 2519–2524.
6. Ladoux,B., Quivy,J.-P., Doyle,P., du Roure,O., Almouzni,G. and Viovy,J.-L. (2000) Fast kinetics of chromatin assembly revealed by single-molecule videomicroscopy and scanning force microscopy. *Proc. Natl Acad. Sci. USA*, **97**, 14251–14256.
7. Murayama,H. and Yoshikawa,K. (1999) Thermodynamics of the collapsing phase transition in a single duplex DNA molecule. *J. Phys. Chem. B*, **103**, 10517–10523.
8. Mel'nikov,S.M., Sergeyev,V.G. and Yoshikawa,K. (1995) Transition of double-stranded DNA chains between rondom coil and compact globule states induced by cooperative binding of cationic surfactant. *J. Am. Chem. Soc.*, **117**, 9951–9956.
9. Gosule,L.C. and Schellman,J.A. (1976) Compaction form of DNA induced by spermidine. *Nature*, **259**, 333–335.
10. Lerman,L.S. (1971) Transition to a compact form of DNA in polymer solutions. *Proc. Natl Acad. Sci. USA*, **68**, 1886–1890.
11. Kwoh,D.Y., Coffin,C.C., Lollo,C.P., Jovenal,J., Banaszczyk,M.G., Mullen,P., Phillips,A., Amini,A., Fabrycki,J., Bartholomew,R.M. *et al.* (1999) Stabiliztion of poly-L-lysine/DNA polyplexes for in vivo gene delivery to the liver. *Biochem. Biophys. Acta*, **1444**, 171–190.
12. Thomas,T. and Thomas,T.J. (2001) Polyamines in cell growth and cell death: molecular mechanism and therapeutic applications. *Cell. Mol. Life Sci.*, **58**, 244–258.
13. Ichikawa,M., Matsuzawa,Y., Koyama,Y. and Yoshikawa,K. (2003) Molecular fabrication : aligning DNA molecules as building blocks. *Langmuir*, **19**, 5444–5447.
14. Hirano,K., Nagata,H., Ishido,T., Tanaka,Y., Baba,Y. and Ishikawa,M. (2008) Sizing of single globular DNA molecules by using a circular acceleration technique with laser trapping. *Anal. Chem.*, **80**, 5197–5202.
15. Matsuura,K., Masumoto,K., Igami,Y., Kim,K. and Kimizuka,N. (2009) CTAB-induced morphological transition of DNA micro-assembly from filled spheres to hollow capsules. *Mol. Biosys.*, **5**, 921–923.
16. Yoshikawa,K., Hirota,S., Makita,N. and Yoshikawa,Y. (2010) Compaction of DNA induced by like-charge protein: opposite salt-effect against the polymer-salt-induced condensation with neutral polymer. *J. Phys. Chem. Lett.*, **1**, 1763–1766.
17. Tsumoto,K., Luckel,F. and Yoshikawa,K. (2003) Giant DNA molecules exhibit on/off switching of transcriptional activity through conformational transition. *Biophys. Chem.*, **106**, 23–29.
18. Yoshikawa,K. and Matsuzawa,Y. (1995) Discrete phase transition of giant DNA dynamics of globule formation from a single molecular chain. *Physica D*, **81**, 220–227.
19. Yoshikawa,K. and Matsuzawa,Y. (1996) Nucleation and glowth in single DNA molecules. *J. Am. Chem. Soc.*, **118**, 929–930.
20. Vasilevskaya,V.V., Khokhlov,A.R., Matsuzawa,Y. and Yoshikawa,K. (1995) Collapse of single DNA molecule in poly(ethylene glycol) solutions. *J. Chem. Phys.*, **102**, 6595–6602.
21. Grosberg,A.Y. and Khoklov,A.R. (1994) *Statistical Physics of Macromolecules*. Academic Institute of Physics, NY.
22. Miyoshi,D. and Sugimoto,N. (2008) Molecular crowding effects on structure and stability of DNA. *Biochimie*, **90**, 1040–1051.
23. Wilson,R.W. and Bloomfield,V.A. (1979) Counterion-induced condensation of deoxyribonucleic acid. A light-scattering study. *Biochemistry*, **18**, 2192–2196.
24. Humpolickova,J., Benda,A., Sykora,J., Machan,R., Kral,T., Gasinska,B., Enderlein,J. and Hof,M. (2008) Equilibrim dynamics of spermine-induced plasmid DNA condensation revealed by fluorescence lifetime correlation spectroscopy. *Biophys. J.*, **94**, L17–L19.
25. Takahashi,M., Yoshikawa,K., Vasilevskaya,V.V. and Khokhlov,A.R. (1997) Discrete coil-globule transition of single duplex DNAs induced by polyamines. *J. Phys. Chem. B*, **101**, 9396–9401.
26. Todd,B.A., Parsegian,V.A., Shirahata,A., Thomas,T.J. and Rau,D.C. (2008) Attractive forces between cation condensed DNA double helices. *Biophys. J.*, **94**, 4775–4782.
27. Donald,C.R. and Parsegian,V.A. (1992) Direct measurement of the intermolecular forces between counterion-condensed DNA double helices. Evidence for long range attractive hydration forces. *Biophys. J.*, **61**, 246–259.
28. Daoud,M., Cotton,J.P., Farnoux,B., Jannink,G., Sarma,G., Benoit,H., Duplessix,R., Picot,C. and de Gennes,P.G. (1975) Solutions of flexible polymers. Neutron experiments and interpretation. *Macromolecules*, **8**, 804–818.